Research Journal of Applied Sciences, Engineering and Technology 4(20): 3937-3942, 2012
ISSN: 2040-7467

Submitted: December 20, 2011 Accepted: April 23, 2012 Published: October 15, 2012

Analytical Design of the Optimal Driving Location for a Novel Ultrasonic Actuator by Zone-Energy Method

Shann-Chyi Mou
Department of Mechanical Engineering, Ching Yun University, Zhongli, 32097 Taiwan

Abstract: This study is proposed with the ideology of zone-energy method to precisely analyze the optimal driving location of novel ultrasonic actuator. This actuator is designed with the piezoelectric buzzer to act as its actuating component. It is formed a 3-phase continuous traveling wave by using the asymmetric framework within the metal plate, it is therefore accessible to actuate the shaft. In order to produce the congruent driving force caused by 3-phase continuous traveling waves within a periodic pulse, the optimal driving location must be situated on the eccentric location of buzzer instead of its core. The zone-energy method, in view of the energy balance, is available to find out the location of eccentric screw. By using this method, it is aimed to precisely solve out the optimal driving location that is situated on the a-third wavelength distance away from the circle center and the offset angle of 30ºC apart from a certain screw on the Ni-alloy plate.

Keywords: Piezoelectric buzzer, ultrasonic actuator, zone-energy method

INTRODUCTION

Currently there are numerous ultrasonic actuators or actuators are manufactured by using the stack piezoelectric materials. Thus, the cost is expensive and the structure is unable to be flat and slim (Sashida and Kenjo, 1993; Ueha *et al*., 1993; Uchino, 1997). In 2004, Wen *et al*. (2004), Mou and Ouyang (2004) proposed to employ the piezoelectric buzzer to construct a novel ultrasonic actuator. Figure 1 shows the said stator structure for his designed shaft-driving type ultrasonic actuator. The Ni-alloy plate of buzzer is respectively and equivalently fastened with screws at the angle of 120ºC (Idogaki *et al*., 1996). Also, on the eccentric location of piezoelectric membrane, they are all fastened with the screws of the same type as well. When the voltage is powered onto the buzzer, due to converse piezoelectric effect, it will make piezoelectric material cause the fluctuation along both the radial and arc directions. Because of the fact that it will form a reflection point during the wave propagation of screws, thus, the reflection formed by 3 screws on the metal plate will reflect the waves back to its circle center. It is shown in Fig. 1. Knowing from the simulation diagram of ANSYS (finite element analysis software) shown in Fig. 2 (Ye and Ouyang, 1990), if we place the driving point onto the circle center of piezoelectric buzzer, the reflection wave formed by 3 screws, will reach the circle center simultaneously. The elliptical motion trajectory on the circle center cannot be generated through the 3-phase continuous traveling waves. Namely, the symmetric structure formed by screws is a conservation filed which cannot transmit the energy outward. Obviously, the circle center is entirely a motionless point in Fig. 2.

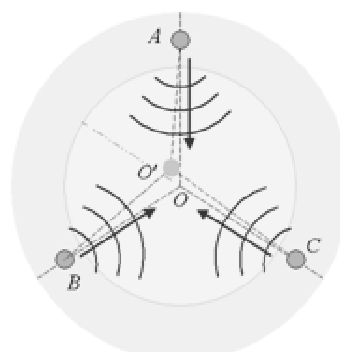

Fig. 1: The structure diagram of a novel ultrasonic motor

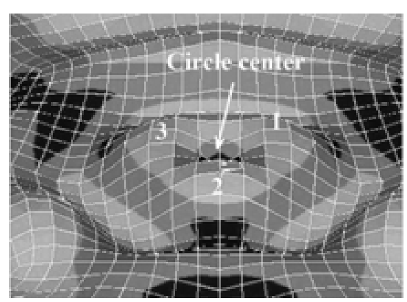

Fig. 2: The dynamic simulation diagram of neighboring area for circle center by ANSYS

Because the symmetric structure will cause the mutual counteraction for the energy of 3-phase traveling waves, it is required to equip with an additionally designed eccentric point to shape up the asymmetric structure accordingly. The eccentric screw is aimed to

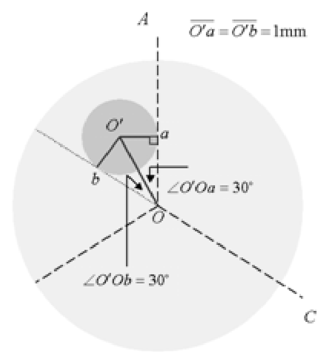

Fig. 3: The partial zoom-in diagram of Fig. 1

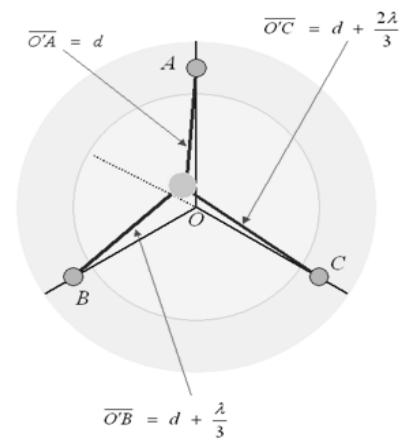

Fig. 4: The relational location diagram for screws on buzzer

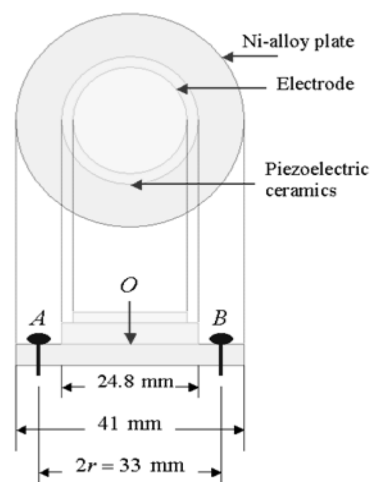

Fig. 5: The dimension diagram of piezoelectric buzzer

differ from the reflection routes when the three energy waves return to the eccentric point. It also means that when each reflection wave reaching the eccentric point, it will slightly cause phase difference. It is therefore available to evade the counteraction when reflection waves arriving the circle center to result in the actuation failure.

We will make the RPM measurement for the piezoelectric buzzer at its different locations. The highest rotational speed can be treated as the basis to search for the optimal driving location. Through the experiment results, we can roughly estimate the location of eccentric screw which are thought to be at a-third wavelength distance away from its circle center and the offset angle of 30˚C apart from a certain screw on the Ni-alloy plate. On the practical production of actuator, the screw is an exact dimension of 2 mm diameter not an infinitesimal point, it will be definitely to exist in the working error. The practical produced piece is directly designed with the location of eccentric screw shown as Fig. 3. Figure 3 is the partial zoom-in illustration of Fig. 1 including the adjacent area of circle center O and eccentric point O . The outer rim of eccentric screw is exactly tangent to both lines of OA and Cb (Cb is the extended line of CO). So, the location of eccentric point O is finally determined. Knowing form Fig. 3, OO = 2 mm, namely, during the practical working process, the distance from eccentric screw to its circle center is around 2 mm.

By method of trial and error, it is not so objective for us to well search for the optimal driving location. It merely comes with the qualitative explanation but no quantitative description and lacking in reasonable mathematic deduction and theoretical interpretation. Thus, this article is aimed to employ the numerical analytics to precisely solve out the optimal driving location of shaft-driving type ultrasonic actuator.

Assumptions and definitions:

- Assume the cross-sectional area of screw can be ignored, namely, any given screw location can viewed as a point. We also define the 3 points of A, B and C to treat as the screw location of metal plate on buzzer. It is shown in Fig. 4.
- The circle center location of piezoelectric buzzer is defined as point O and r means the interval distance from O to A, B and C. Clearly, the r is about 16.5 mm according to Fig. 5. It is especially noteworthy that r is not exactly the radius of piezoelectric buzzer.
- The location of eccentric screw is defined as point O and it also means the optimal driving location. The selection of O must leave O A, O B and O C with the unequal distances mutually. In order to simplify the situation, we assume the distance relation of O A<O B<O C with the correspondingly relative locations shown on Fig. 4.
- λ is defined as the wavelength of traveling wave on piezoelectric buzzer. Seeing form the carbon powder pattern (Wen *et al*., 2004, 2003) within Fig. 6 and the ANSYS simulation diagram in Fig. 7, it is available

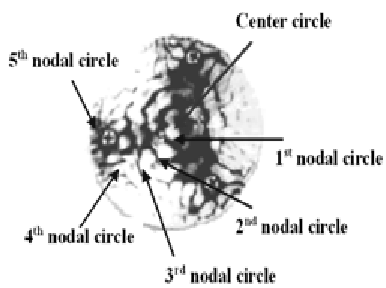

Fig. 6: The carbon powder pattern of piezoelectric buzzer

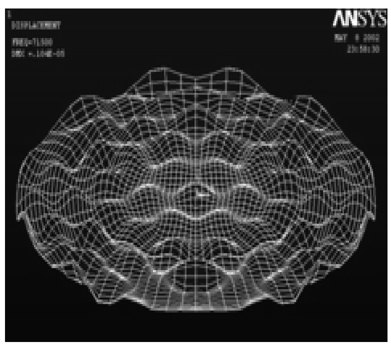

Fig. 7: The ANSYS simulation diagram of piezoelectric buzzer

to calculate that the value of λ approximates to 3.72 mm.

- d is defined as the distance of segment O A. If N is an positive integral, then O A = d = N × λ. It means that the distance of O A is N folds of wavelength. In a periodic pulse, through eccentric screw, will create 3 runs of continuously driving traveling waves. It can be equally held that the λ is evenly divided into 3 fractions at the equivalent angle 120ºC respectively with the 3-phase rational mechanism. The distances from O to 3 screws are separately shown as d, d + (λ/3) and d + (2λ/3) in order. In another word, O B = d + (λ/3) and O C = d + (2λ/3), with the correlative locations illustrated in Fig. 4.
- Assume the distance is λ/3 between O to O, namely point O placing right on the circle with the radius of λ/3. It is shown in Fig. 8. θ is defined as an included angle between OO and OA. In response to the hypothesis of O A<O B<O C mentioned in the item 3, we mainly hope to simplify the solution that point O can be distributed within the range of ∠AOB.

DRAWING METHODOLOGY

Step 1: It have known that d = N × λ. Let N = 1 to make d = 3.72 mm, then d + (λ/3) = 4.96 mm and d + (2λ/3) = 6.20 mm. In Fig. 9, 3 circles are,

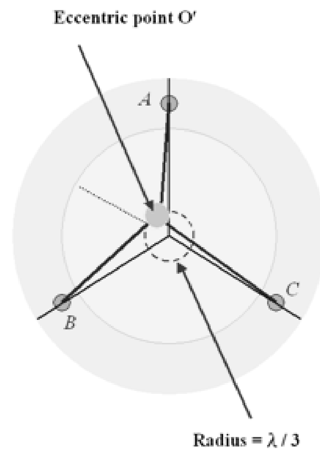

Fig. 8: The relational location diagram of eccentric screw

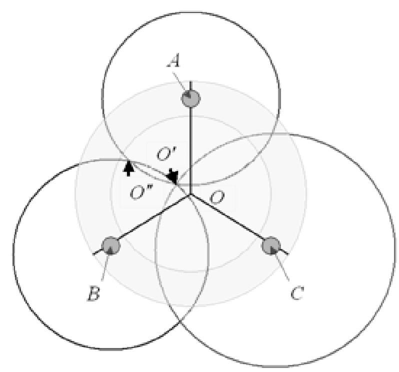

Fig. 9: He concept diagram of drawing method

respectively depicted to take A, B and C as the circle centers with the radiuses of O A, O B and O C.

Step 2: If the foresaid 3 circles never insect mutually, the process must back to the step 1 with the N enlarged to 2. At this moment, O A = 7.44 mm, O B = 8.68 mm and O C = 9.92 mm. Again, the 3 circles are depicted with the new radiuses of O A, O B and O C to inspect the possible of intersection between 3 circles.

Step 3: Increasing with the N value, it will gradually appear the intersection between any 2 circles. Based on the assumption of O A<O B<O C, if it is available for 3 circles commonly insect right on a point within the range of ∠AOB, then this so-called intersection point will be exactly the correct location of point O . The O out of the range within ∠AOB is not a correct location, otherwise.

Step 4: To keep on increasing with the N value, the point intersected by 3 circles will occur in the range of ∠AOB. This intersection point will be exactly the

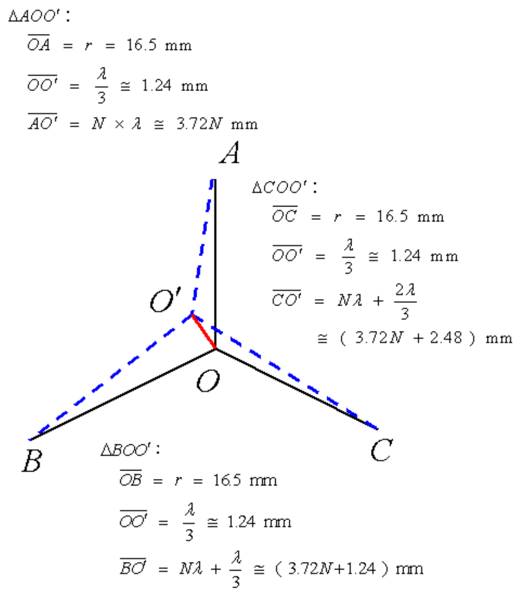

Fig. 10: The concept diagram of zone-energy method

location of eccentric screw and ∠AOO is defined as the eccentric angle of point O , denoted as θ. In Fig. 9, because point O is merely intersected by 2 circles within the range of ∠AOB, it is not the valid eccentric point.

Zone-energy method: In Fig. 4, the correlative region of A, B, C, O and O is redraw to show as Fig. 10. Seeing from the figure, the 5 points form 3 respective triangle formations of ▵AOO , ▵BOO and ▵COO . Because each side length of these 3 triangles have been known, thus, the areas of $A_{\triangle AOO}$, $A_{\triangle BOO}$ and $A_{\triangle COO}$ can be separately solved by using the Heron's formula (Foerster, 1999) (shown as below (1), (2) and (3)):

$$S_1 \equiv \frac{\overline{OA}+\overline{OO'}+\overline{OA'}}{2} = \frac{17.74+3.72N}{2}$$
$$A_{\Delta AOO'} = \sqrt{S_1\left(S_1-\overline{OA}\right)\left(S_1-\overline{OO'}\right)\left(S_1-\overline{AO'}\right)} \quad (1)$$

$$S_2 \equiv \frac{\overline{OB}+\overline{OO'}+\overline{OB'}}{2} = \frac{18.98+3.72N}{2}$$
$$A\Delta BOO' = \sqrt{S_2\left(S_2-\overline{OB}\right)\left(S_2-\overline{OO'}\right)\left(S_2-\overline{OB'}\right)} \quad (2)$$

$$S_3 = \frac{\overline{OC}+\overline{OO'}+\overline{CO'}}{2} = \frac{20.22 = 3.72N}{2}$$
$$A_{\Delta COO'} = \sqrt{S_3\left(S_3-\overline{OC}\right)\left(S_3-\overline{OO'}\right)\left(S_3-\overline{CO'}\right)} \quad (3)$$

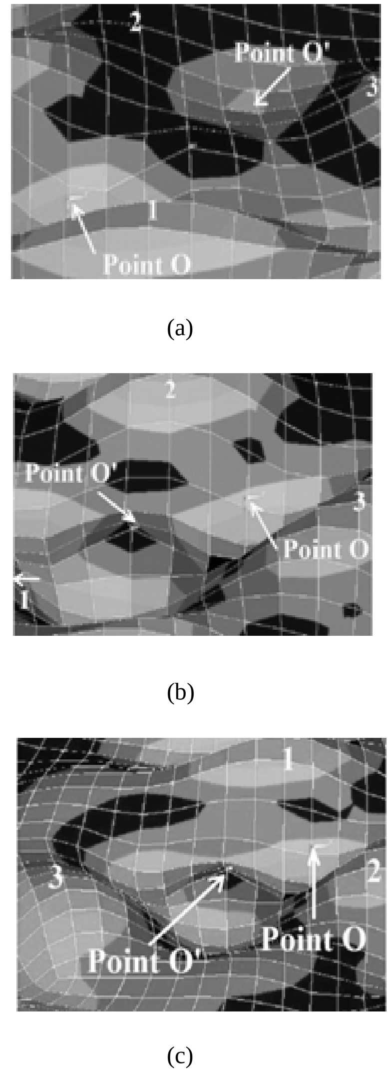

Fig. 11: The simulation diagram of neighboring area for eccentric point O'

The eccentric screw is mainly designed with the purpose that within a periodic pulse, it can continuously create 3-phase traveling waves with the congruent driving force.

In view of the energy balance, obviously, the areas of ▵AOO, ▵BOO and ▵COO must be all equal. The equation of $A_{\triangle AOO} = A_{\triangle BOO} = A_{\triangle COO}$ can be divided into 3 partial equations of $A_{\triangle AOO} = A_{\triangle BOO}$, $A_{\triangle BOO} = A_{\triangle COO}$ and $A_{\triangle AOO} = A_{\triangle COO}$. The (1), (2) and (3) are substituted into the triangular relational equations to find out the N value. If the unique solution of $A_{\triangle AOO} = A_{\triangle BOO} = A_{\triangle COO}$ is existed, then, any 2 of the above-said 3 equations can be well solved out for the deduction sufficiently. The answer of N value can be solved and the results are shown in (4) by using the computer software-Mathematica:

$$\begin{cases} A_{\Delta AOO'} = A_{\Delta BOO'} \Rightarrow \\ \quad N = -4.61153, -0.166667, 4.2782 \\ A_{\Delta BOO'} = A_{\Delta COO'} \Rightarrow \\ \quad N = -4.94487, -0.53.94487 \\ A_{\Delta AOO'} = A_{\Delta COO'} \Rightarrow \\ \quad N = -4.76882, -0.333333, 4.10215 \end{cases} \tag{4}$$

Simulation and verification: he neighboring area of eccentric point O is simulated by ANSYS software. Figure 11a, b and c (Ye and Ouyang, 1990) show the simulation results of 3 different timings in the same cycle. Clearly, the 3-phase traveling waves surrounding point O occur the gyration with the available actuating force for shaft.

RESULTS AND DISCUSSION

The eccentric location of point O can be found easily by using the drawing method, but it causes the possible outcomes mentioned as below. When N increases continuously to cause d>r, it is never available for the intersected point by 3 circles with the range of ∠AOB. It does not mean within the range of ∠AOB, the piezoelectric buzzer will exist in no any given O and it is because of the limited frequency for drawing. The introduction of variable N and the limitation of positive integral are aimed to reduce the drawing frequency. So, within the range of ∠AOB, the unavailability to find the point O is merely due to the fact that this point is exactly falling on the location of non-integral for N. The N value should be modified as the positive real number (unnecessary positive integral). From the solved result with (4), we find that it is unavailable to find a valid N simultaneously meet the conditions of $A_{\Delta AOO} = A_{\Delta BOO}$, $A_{\Delta BOO} = A_{\Delta COO}$ and $A_{\Delta AOO} = A_{\Delta COO}$. However, these 3 positive N values (invalid for negative value) approximate one another with the values within the narrow range from 3.94487 to 4.27820. The failure for 3 N values further approximating (a unique solution) is impeded by the estimated error of wavelength λ. Observing from the narrow range between 3.94487 and 4.27820, the estimated wavelength of foresaid carbon powder pattern will be correct and reasonable.

Because the point O is defined in the range of ∠AOB and confined by the unavailability for re-estimating, the more right selection of N value must be based the solution from $A_{\Delta AOO} = A_{\Delta BOO}$ (N = 4.2782) of (4) to decide. Compromise to the influence caused by 2 conditions of $A_{\Delta BOO} = A_{\Delta COO}$ and $A_{\Delta AOO} = A_{\Delta COO}$, therefore N = 4.20 is selected as the reason to solve the eccentric angle θ. The proportion of ΔAOO within Fig. 10 is redrawn into Fig. 12. Among them, θ =∠AOO =∠AO X = Cos^{-1}(h/d). N = 4.20 will be substituted into the (1) and the area equivalence correlation of (5) is employed to find out the fact that h = 0.8537 mm and θ = 86.8678ºC:

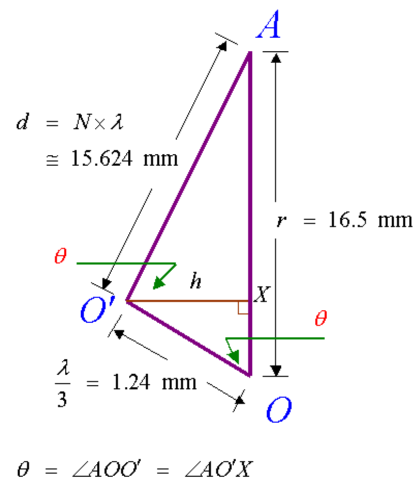

Fig. 12: The concept diagram of eccentric

$$\begin{aligned} &\because A_{\Delta AOO'}\Big|_{N=4.20} = \frac{r \times h}{2} = \frac{16.5}{2} = 7.0429 \\ &\because\Rightarrow h = \frac{7.0429 \times 2}{16.5} \cong 0.8537 mm \end{aligned} \tag{5}$$

Because the piezoelectric buzzer has been evenly divided into 3 proportions, thus, based on the symmetry, the eccentric point O can be availably placed within any range of ∠AOB, ∠BOC or ∠AOC. The assumption of O A<O B<O C mainly meant to simplify the number of solution for N. If this constraint is eliminated, the point O will place at the complementary angle, namely the location of θ = 120-86.8678ºC = 33.1322ºC. This result is almost as the deduction of Fig. 3 for shaft-driving type ultrasonic actuator.

CONCLUSION

In this article, the subject is adopted with the novel ultrasonic actuator constructed by the piezoelectric buzzer and it is also featured with comprehensive mechanism design, affordable price, speedy RPM and smart dimension, typically filled with future development tendency and adoptability. The ultrasonic actuator or actuator is ordinarily defected with low output efficiency (electromechanical coupling factor). The vulnerable effect caused by the drift of system resonant frequency (load change of rotor), the mal-design of driving location and other potential factors. Therefore, it will further deteriorate the system efficiency to impede the output torque and rotational speed. Based on the fact that the 3-phase continuous traveling waves will provide the congruent driving force in a periodic pulse, thus, it is available to find out the location of eccentric screw from the concept of the energy balance. The ideology of zone-energy method has been well proposed in the analysis procedures for the optimal driving location of actuator. With the notion that equivalent area will mean the energy balance, the optimal driving location of actuator can be precisely deduced. It is quite conform to the theoretical deduction and the experimental observation by trial and error method. The solved result of optimal driving location will be considerably beneficiary for the optimal structure deign of actuator system, improvement of output efficiency, the mitigation of temperature rising, system control and stability of dynamic characteristic, etc.

REFERENCES

Foerster, P.A., 1999. Algebra and Trigonometry: Functions and Applications. 2nd Edn., Addison-Wesley, Menlo Park, Calif.

Idogaki, T., T. Tominaga, K. Senda, N. Ohya and T. Hattori, 1996. Bending and expending motion actuators. Sens. Actuat. Phys., 54(3): 760-764.

Mou, S.C. and M.S. Ouyang, 2004. Design, simulation, modeling and analysis of a shaft-driving type ultrasonic motor. Ph.D. Thesis, National Tsing Hua University, Taiwan, pp: 90-117.

Sashida, T. and T. Kenjo, 1993. An Introduction to Ultrasonic Motors. Clarendon Press, Oxford, pp: 17-23.

Uchino, K., 1997. Piezoelectric Actuators and Ultrasonic Motors. Kluwer Academic Publishers, Boston, pp: 265-267.

Ueha, S., Y. Tomikawa, M. Kurosawa and N. Nakamura, 1993. Ultrasonic Motors-Theory and Applications. Clarendon Press, Oxford, pp: 4-7.

Wen, F.L., C.Y. Yen and M.S. Ouyang, 2003. Thin-disk piezoceramic ultrasonic motor. Part I: design and performance evaluation. Ultrasonics, 41: 437-450.

Wen, F.L., S.C. Mou and M.S. Ouyang, 2004. Design and construction of shaft-driving type piezoceramic ultrasonic motor. Ultrasonics, 43: 35-47.

Ye, J.Y. and M.S. Ouyang, 1990. Design and simulation of disk type ultrasonic actuator. MA. Thesis, National Tsing Hua University, Taiwan, pp: 37-41.